



The role of niobia location on the acidic and catalytic functionalities of heteropoly tungstate

Ch. Ramesh Kumar^a, S. Gatla^b, O. Mathon^b, S. Pascarelli^b, N. Lingaiah^{a,*}

^a *Catalysis Laboratory, Inorganic & Physical Chemistry Division, CSIR-Indian Institute of Chemical Technology, Hyderabad, Telangana 500 007, India*

^b *Electronic Structure and Magnetism (ESM) Group, European Synchrotron Radiation Facility (ESRF) 71, Avenue des Martyrs, 38000 Grenoble, France*



ARTICLE INFO

Article history:

Received 9 March 2015

Received in revised form 17 June 2015

Accepted 19 June 2015

Available online 23 June 2015

Keywords:

Anisole

Benzyl alcohol

Dibenzylether

Keggin ion

Niobium

Heteropoly tungstate

ABSTRACT

12-Tungstophosphoric acid (TPA) was modified systematically by incorporating niobium into its primary and secondary structure. TPA supported on niobia catalyst was also prepared by impregnation method. These catalysts were characterized by FT-infrared, X-ray diffraction, Laser Raman, X-ray photoelectron spectroscopy, X-ray absorption spectroscopy, UV-vis diffuse reflectance spectroscopy, solid state ³¹P nuclear magnetic resonance spectroscopy, temperature programmed desorption of ammonia and pyridine adsorbed FT-IR spectroscopy. Characterization results suggest the presence of intact Keggin structure after modification of parent TPA. Incorporation of Nb into the secondary structure results in generation of Lewis acidic sites. Nb containing TPA catalysts exhibited high acidity compared to the TPA supported on niobia catalyst. The activity of the catalysts was evaluated for benzylation of anisole with benzyl alcohol. Catalyst activity depended on the location of niobium ion in the heteropoly tungstate.

© 2015 Elsevier B.V. All rights reserved.

1. Introduction

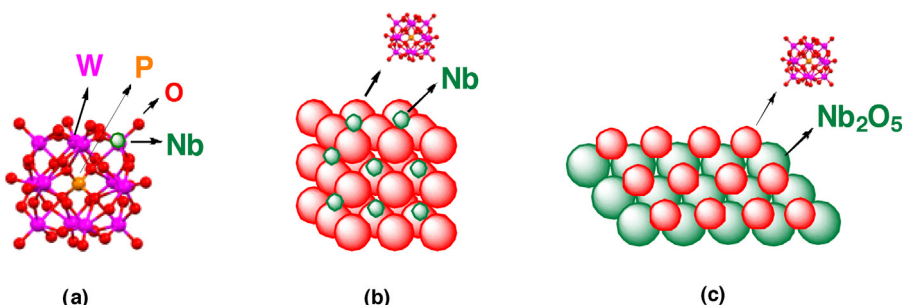
Polyoxometalates (POMs) are composed of early transition-metals of group V and VI in their highest oxidation states [1]. POMs are classified into two categories, namely isopolyoxometalates and heteropolyoxometalates. Among the heteropolyoxometalates, Keggin type are the most frequently used in catalysis, represented by the formula $[XM_{12}O_{40}]^{n-}$. The Keggin anion is made of an assembly of twelve MO_6 octahedrons sharing their corners or edges with a central XO_4 tetrahedron, where X is a hetero atom (P^{5+} , Si^{4+}), n is the oxidation state and M is the addenda atom (Mo^{6+} , W^{6+} , V^{5+}). The metal oxide cluster molecule $[XM_{12}O_{40}]^{n-}$ is called as primary structure. Secondary structure is a regular arrangement of poly anions counter cations and also some polar molecule such as water [2]. The catalytic properties of heteropoly acids (HPAs) can be tuned in a systematic way by exchanging counter-cations and hetero atoms [3–6]. Park et al. studied the acidic and oxidation properties of HPA catalysts by exchanging the identity of addenda atom with group-V metal ions such as V^{5+} , Nb^{5+} and Ta^{5+} [7–9].

The acidic and redox properties of the modified HPA catalysts depend on the nature of metal ion and its location in Keggin ion. HPAs with incorporation of V into its primary structure were reported [7,10]. This modification resulted in the increase of the redox nature of HPAs particularly heteropoly molybdate for different oxidation reactions [11–13]. The modification of HPAs by incorporating different metal ions in their primary and secondary structures will totally provide new catalytic functionalities. It is anticipated that by modifying the heteropoly tungstate which is the strongest acid among the HPAs by different metal ions such as Nb will result in much stronger acidic catalysts. Niobia is known for its acidic behavior and expected to modify the acidity and stability of HPA to a great extent.

In the present work, the role of niobium in the heteropoly tungstate is investigated by preparing (i) incorporation of niobium in the primary structure of Keggin ion of heteropoly tungstate (TPANb₁), (ii) incorporation of niobium in the secondary structure i.e., substitution of counter cations (H^+) of TPA with niobium ($Nb_{0.6}TPA$) and (iii) TPA supported on Nb_2O_5 (25% TPA/ Nb_2O_5) as illustrated in Scheme 1. These catalysts are characterized by different techniques to derive their surface, structural and acidic properties. The catalysts were evaluated for their catalytic activity by taking benzylation of anisole with benzyl alcohol as a

* Corresponding author. Fax: +91 40 27160921.

E-mail address: nakkalingaiah@iict.res.in (N. Lingaiah).



Scheme 1. Structure of (a) niobium incorporated Keggin ion (TPANb₁ or [PW₁₁Nb₁O₄₀]⁴⁻), (b) niobium salt of tungstophosphoric acid (Nb_{0.6}TPA or Nb_{0.6}PW₁₂O₄₀), and (c) tungstophosphoric acid supported on niobia (25% TPA/Nb₂O₅ or 25% H₃PW₁₂O₄₀/Nb₂O₅).

model reaction. The influence of different benzylating agents is also studied.

2. Experimental

2.1. Catalyst preparation

Nb_{0.6}TPA catalyst was prepared as following. 5 g of TPA was dissolved in distilled water and 0.56 g of niobium oxalate dissolved in 0.1 M oxalic acid solution was added to aqueous solution of TPA with continuous stirring. The resultant mixture was stirred for 3 h. Excess water was evaporated on a water bath and the dried catalyst mass was kept for further drying in an air oven for overnight. Finally the sample was calcined at 300 °C for 2 h.

TPANb₁ catalyst was prepared according to the procedure reported in the literature [7]. In a typical procedure, 10 g of niobium oxalate was dissolved in 100 ml of 0.1 M oxalic acid solution and 6 g of Na₂HPO₄ was dissolved in 100 ml of distilled water. These two solutions were mixed together. 100 g of Na₂WO₄·2H₂O was dissolved in 150 ml of distilled water, and subsequently added to the solution containing niobium and phosphorous precursors with vigorous stirring. After heating the resulting solution to 80 °C, 60 ml of H₂SO₄ was slowly added to it. The solution was further kept for reflux at 80 °C for 8 h. After cooling the solution to room temperature, the formed TPANb₁ was extracted with diethyl ether. The resulting etherate was maintained at 50 °C to obtain solid product, dried in an oven and calcined at 300 °C for 2 h.

TPA supported niobium oxide catalyst was prepared by impregnation method. In a typical procedure, required amount of TPA was dissolved in water and this solution was added to niobium oxide with continuous stirring. The resultant mixture was allowed to stand for 3 h and excess water was evaporated on a water bath. The catalyst was kept overnight for drying in an air oven at 120 °C and finally calcined at 300 °C for 2 h. The TPA content on niobia is kept as 25 wt%. The catalyst is denoted as 25% TPA/Nb₂O₅.

2.2. Characterization of catalysts

The FT-IR spectra were recorded on a Bio-Rad Excalibur series spectrometer using the KBr disc method.

The nature of the acid sites (Bronsted and Lewis) of the catalyst samples was determined by FT-IR spectroscopy with chemisorbed pyridine. The pyridine adsorption studies were carried out in the diffuse reflectance infrared Fourier transform (DRIFT) mode. Prior to the pyridine adsorption catalysts samples were degassed under vacuum at 200 °C for 3 h and exposed to dry pyridine. Then, the excess pyridine was removed by heating the sample at 120 °C. After cooling the sample to room temperature, FT-IR spectra of the pyridine-adsorbed samples were recorded. X-ray powder diffraction (XRD) patterns were recorded on a Rigaku Miniflex diffractometer using Cu K_α radiation (1.5406 Å) at 40 kV and 30 mA

and secondary graphite monochromatic. The measurements were obtained in steps of 0.045° with count times of 0.5 s, in the 2θ range of 2–80°.

Confocal micro-Raman spectra were recorded at room temperature in the range of 200–1200 cm⁻¹ using a Horiba Jobin-Yvon Lab Ram HR spectrometer with a 17 mW internal He-Ne (Helium-Neon) laser source of excitation wavelength of 632.8 nm. The catalyst samples in powder form (about 5–10 mg) were loosely spread onto a glass slide below the confocal microscope for measurements.

The acidity of the catalysts was measured by temperature programmed desorption (TPD) of ammonia. In a typical experiment, 0.1 g of catalyst was loaded and pre-treated in He gas at 300 °C for 2 h. After pre-treatment the temperature was brought to 100 °C and the adsorption of NH₃ was carried out by passing a mixture of 10% NH₃ balanced He gas over the catalyst for 1 h. The catalyst surface was flushed with helium gas at the same temperature for 2 h to flush off the physisorbed NH₃. TPD of NH₃ was carried with a temperature ramp of 10 °C/min and the desorbed ammonia was monitored using thermal conductivity detector (TCD) of a gas chromatograph.

X-ray photo electron spectroscopy (XPS) measurements were conducted on a KRATOS AXIS 165 with a DUAL anode (Mg and Al) apparatus using Mg K_α anode. The non-monochromatized Al K_α X-ray source ($h\nu = 1486.6$ eV) was operated at 12.5 kV and 16 mA. Before acquisition of the data each sample was out-gassed for about 3 h at 100 °C under vacuum of 1.0×10^{-7} T to minimize surface contamination. The XPS instrument was calibrated using Au as standard. For energy calibration, the carbon 1s photoelectron line was used. The carbon 1s binding energy was taken as 285 eV. Charge neutralization of 2 eV was used to balance the charge up of the sample. The spectra were deconvoluted using Sun Solaris Vision-2 curve resolver. The location and the full width at half maximum (FWHM) value for the species were first determined using the spectrum of a pure sample. Symmetric Gaussian shapes were used in all cases. Binding energies for identical samples were, in general, reproducible within ± 0.1 eV.

The X-ray absorptions (XAS) experiments were performed at the Nb K edge (18.986 KeV) at the BM23 beam line at the European Synchrotron Radiation Facility (ESRF, Grenoble). Monochromatic X-ray beam was obtained from the white beam by using Si(1 1 1) double crystal; a harmonic rejection has been performed using Si coated mirrors. Both the incident (I_0) and transmitted (I_1) monochromatic beam intensities were measured by using ionic chambers filled with 0.65 bar Ar and 2.1 bar Ar, respectively, and eventually I_0 filled up to 2 bar with He. The photon energy was calibrated with the edge energy obtained from the maxima first derivative of the Nb K-edge in the Nb foil (18.986 KeV). The reference samples (Nb foil, Nb₂O₅) were measured in transmission mode. Nb₂O₅ is according to <http://ixs.iit.edu/database> For the TPANb₁, Nb_{0.6}TPA and 25% TPA/Nb₂O₅ samples measurements were done in fluorescence mode with a 13-element Ge detector (Canberra Industries). The extraction of the

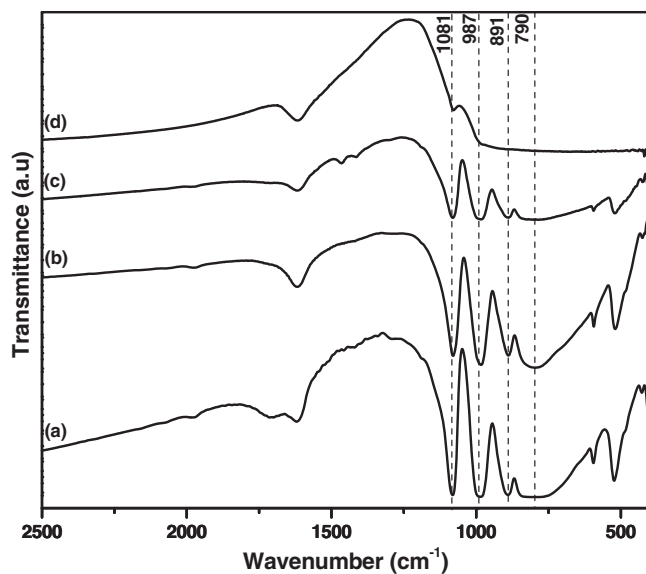


Fig. 1. FT-IR spectra of (a) TPA, (b) TPANb₁, (c) Nb_{0.6}TPA, and (d) 25% TPA/Nb₂O₅ catalysts.

EXAFS $\chi(k)$ function has been done using Athena. Fourier transform of EXAFS function $\chi(k)$ into R space with k^2 weighted factor and Kaiser-Bessel window function has been performed in 2–10 Å⁻¹, a function $|\chi(R)|$ (Å⁻³).

The UV-vis diffuse reflectance spectra (UV-vis DRS) were recorded on a GBC UV-visible Cintra 10e spectrometer in the range of 200–800 nm.

³¹P nuclear magnetic resonance (NMR) spectra of solids were recorded in a 400 MHz Bruker spectrometer. A 4.5 μ s pulse (90°) was used with repetition time of 5 s between pulses in order to avoid saturation effects. Spinning rate was 5 kHz. All the measurements were carried out at room temperature using 85% H₃PO₄ as standard reference.

2.3. General alkylation reaction procedure

The alkylation reaction was carried out in a 50 ml two-necked round bottom flask provided with a reflux condenser with nitrogen inlet and a septum for sample removal. In a typical run, 10 g of anisole and 3.37 g of benzyl alcohol (or 3.08 g dibenzylether) along with 0.1 g catalyst were taken. The reaction was carried out at a reaction temperature of 120 °C under nitrogen atmospheric condition. The reaction mixture was withdrawn at different intervals and analyzed by gas chromatography (VARIAN GC-3800) equipped with a SE-30 column and flame ionization detector. The identification of products was made from GC-MS (SHIMADZU-2010) analysis.

3. Results and discussion

3.1. FT-IR spectroscopy

FT-IR spectra of the catalysts are presented in Fig. 1. All the catalysts showed the characteristic bands of Keggin ion in its finger print region of 500–1200 cm⁻¹ [8,14]. The bands observed at 1081 and 987 cm⁻¹ are related to stretching vibrations of P–O and W=O_t bonds of Keggin ion. Additionally, the bands present at 891 and 790 cm⁻¹ are associated to M–O_c–M and M–O_e–M bonds. All these four characteristic bands of Keggin ion are noticed in the TPANb₁ and Nb_{0.6}TPA samples indicating the retention of Keggin ion structure. However, this is not the situation in the impregnated 25% TPA/Nb₂O₅ sample. Instead, the bands related to Keggin ion are

dominated by the IR spectrum of niobia support to large extent. This is because of strong absorption of niobia in the same infrared region of Keggin ion [15]. Even so, the absorption bands at 1081 and 987 cm⁻¹ still appeared, however, with low intensity suggesting the presence of Keggin ion on niobia support.

3.2. X-ray diffraction patterns

XRD patterns of the samples are shown in Supplementary information as Fig. S1. The patterns of parent TPA are also included for the sake of comparison. TPANb₁ and Nb_{0.6}TPA catalysts showed the most intense peaks at 2θ of 10.2°, 25.4° and 33.5° which are characteristic patterns of Keggin heteropoly acid. No pattern related to niobia was observed in the case of TPANb₁ and Nb_{0.6}TPA catalysts. These results indicate the successful formation of TPANb₁ and Nb_{0.6}TPA Keggin ions [16]. In the supported catalyst weak diffraction peaks of Keggin ion were observed at 2θ of 10.2°, 25.4°, 33.5°. Caliman et al. reported that the catalyst up to 40 wt% of TPA on niobia and calcined below 450 °C shows only characteristic peaks of niobia [15]. Similar result was observed in the case of 25% TPA/Nb₂O₅ catalyst. These results substantiate that exchanging the protons of TPA with Nb⁵⁺ ion and incorporation of Nb⁵⁺ in the primary Keggin structure of heteropoly anion do not alter the Keggin structure of heteropoly tungstate.

3.3. Laser Raman spectra

Laser Raman spectra of the catalysts along with spectra of parent TPA are also presented in Supplementary information (Fig. S2). Nb_{0.6}TPA and TPANb₁ catalysts showed characteristic bands at 991, 1010 cm⁻¹ corresponding to asymmetric and symmetric stretching of W=O_t of TPA [15,17]. In the case of 25% TPA/Nb₂O₅ sample, less intense bands related to symmetric stretching frequency of W=O_t are noticed due to amorphous nature of niobia and lower loading amount of TPA on niobia. Caliman et al. reported that with increased amount of tungstophosphoric acid on niobia, the Keggin peaks became more intense and well defined [15]. In case of TPANb₁ and Nb_{0.6}TPA, the peak in the range of 700–800 cm⁻¹ related to WO₃ (decomposition product of TPA) is absent indicating the stability of TPA structure. These results point to the incorporation of Nb⁵⁺ into the structure of heteropoly tungstate. Supporting of TPA on niobia also does not cause any decomposition of Keggin ion but reduced the intensity of the peaks. Besides, a strong band centered at ca. 700 cm⁻¹ generated, associated to the stretching modes of different niobia polyhedra [15,18]. These results are in accordance with those obtained by FT-IR and XRD.

3.3.1. In-situ laser Raman spectra

In order to know the structural changes during the calcination in niobium containing heteropoly tungstate, Nb_{0.6}TPA and TPANb₁ catalysts were subjected to in-situ Raman studies during calcination. The spectra were recorded in-situ at various temperatures ranging from room temperature to 600 °C. Fig. 2(a) and (b) shows the in-situ Raman spectra of Nb_{0.6}TPA and TPANb₁ catalysts, respectively. Generally Keggin bands of TPA were observed at 1010, 991, 237, 219, 158 and 102 cm⁻¹ [15]. Raman spectra of the samples recorded at room temperature shows bands at 991 and 1010 cm⁻¹ corresponding to asymmetric and symmetric stretching frequencies of W=O_t bond of Keggin ion. Further increase in temperature to 200 °C these bands shifted to higher wave numbers to 1017 cm⁻¹. The shift of W=O_t vibration is due to the loss of crystal water and removal of its hydrogen bonding [10]. On further increase in calcination temperature up to 450 °C, not much variation in the spectra was observed. But marginal changes to the spectra were noticed above 500 °C only. At this temperature, the TPANb₁ catalyst (Fig. 6) showed partial degradation of Keggin ion, whereas destabilization

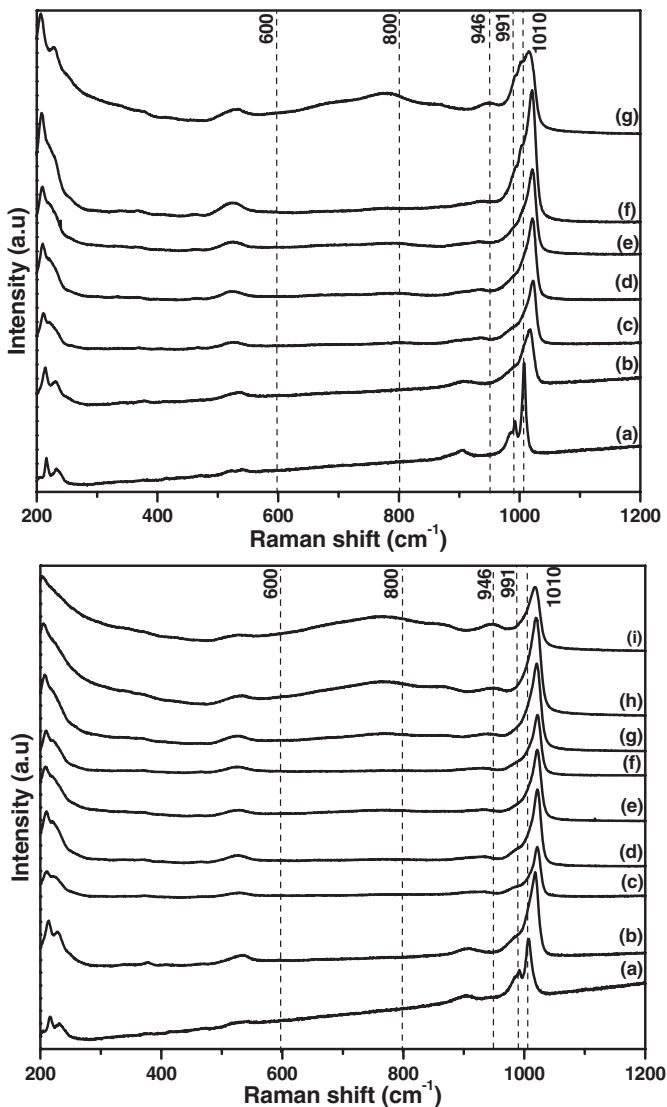


Fig. 2. *In-situ* Raman spectra of (A) Nb_{0.6}TPA (B) TPANb₁ catalysts during exposure to different temperatures (a) RT (b) 200 °C (c) 300 °C (d) 400 °C (e) 450 °C (f) 500 °C (g) 600 °C.

of the Keggin structure is more prominent in Nb_{0.6}TPA catalyst (Fig. 2a). The Raman spectra of Nb_{0.6}TPA sample recorded at 500 °C showed two additional peaks at 946 cm⁻¹ and a broad band in the range of 600–800 cm⁻¹. The band at 946 cm⁻¹ is related to tungsten oxide [19] and the broad band in the range of 600–800 cm⁻¹ is due to niobium oxide [15]. In case of TPANb₁ sample even though the restructuring initiated at 500 °C, the new bonds are apparent only after 550 °C. As a whole, we can say that the Nb incorporated TPA (TPANb₁) catalyst is stable up to 500 °C and the Nb exchanged TPA catalyst (Nb_{0.6}TPA) is slightly less stable than that of TPANb₁.

3.4. Temperature programmed desorption of ammonia

Acidity of the niobium containing heteropoly tungstate samples were measured by TPD of NH₃ experiments. The TPD of ammonia profiles are shown in supplementary information as Fig. S3. The acidity of TPANb₁, Nb_{0.6}TPA and 25% TPA/Nb₂O₅ catalysts were determined from the peak area of desorbed ammonia and summarized in Table 1. The total acidity of the samples is in the following order: TPANb₁ > Nb_{0.6}TPA > 25% TPA/Nb₂O₅. Both the TPANb₁ and Nb_{0.6}TPA catalysts showed strong NH₃ desorption peaks at high temperature (500–700 °C) and low intense desorption peaks in

Table 1
Acidity of TPANb₁, Nb_{0.6}TPA, and 25% TPA/Nb₂O₅ catalysts.

Catalyst	Acidity (mmol/g)		
	Moderate	Strong	Total
TPANb ₁	0.19	—	0.84
Nb _{0.6} TPA	0.18	0.03	0.29
25% TPA/Nb ₂ O ₅	0.29	0.03	0.04
			1.03
			0.50
			0.36

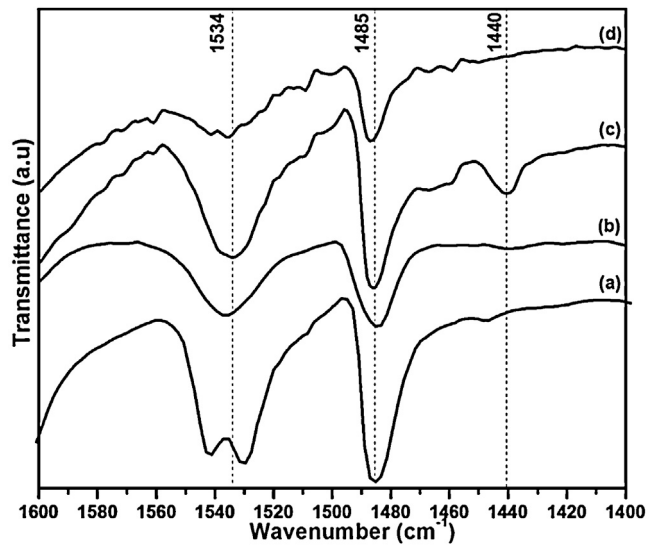


Fig. 3. Pyridine adsorbed FT-IR spectroscopy (a) TPA, (b) TPANb₁, (c) Nb_{0.6}TPA, and (d) 25% TPA/Nb₂O₅ catalysts.

the low temperature (120–350 °C). Conversely, the supported catalyst showed less intense desorption peaks at high temperature but slightly higher intense low temperature peak compare to TPANb₁ and Nb_{0.6}TPA samples. The high temperature desorption peaks are correspond to the strong acidic sites of TPA, whereas low temperature peaks are related to weak acidic sites mainly originated from support niobia. Interestingly, Nb_{0.6}TPA contains another small desorption peak at 410 °C which can be related to moderate Lewis acidic sites. But the strong desorption peak in Nb_{0.6}TPA catalyst was observed at relatively lower temperature (\approx 550 °C) with low intensity compared to its counterpart TPANb₁ (\approx 610 °C). Shifting of this desorption peak to higher temperature point out that TPANb₁ has strong acidic sites [9]. In the case of metal salts of TPA, shift in the desorption peak towards lower temperature is an indication for the exchange of H⁺ ion with the external metal cations [16,17]. Similar situation is noticed in the present Nb_{0.6}TPA catalyst, which specify the substitution of H⁺ by niobium. These results suggests that the catalyst in which Nb is incorporated in to the primary structure of TPA exhibited highest acidity compared to other catalysts as shown in Table 1. These results indicate that the location of Nb influences the acidity of Nb containing TPA catalysts.

3.5. Pyridine adsorbed FT-IR spectroscopy

Pyridine adsorbed FT-IR spectra of niobium containing catalysts were recorded and the results are shown in Fig. 3. The pyridine adsorbed FT-IR spectra showed various features in the region of 1400–1600 cm⁻¹ due to the stretching vibrations of M–N (metal–nitrogen) and N–H (pyridinium ion). The bands at 1536 cm⁻¹ corresponds to Bronsted acidic sites and band related to Lewis acidic sites appeared at 1440 cm⁻¹. All the catalysts contain bands at 1534 and 1485 cm⁻¹ related to Bronsted acidic sites [20]. However, Nb_{0.6}TPA catalyst exhibited one more band at 1440 cm⁻¹ corresponding to Lewis acidic sites. This is due to presence of Nb

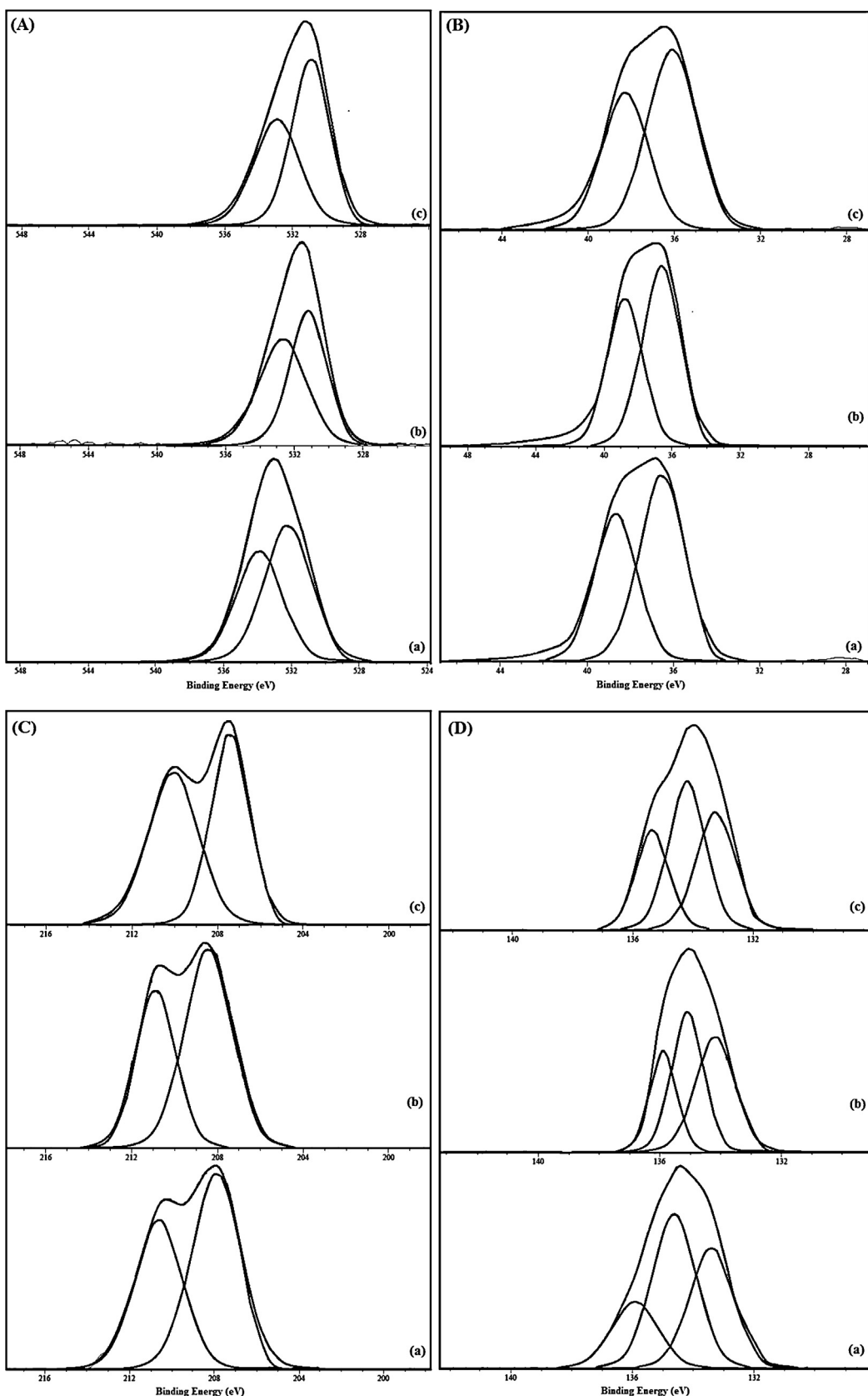


Fig. 4. X-ray photo electron spectroscopy profiles of (A) O 1s, (B) W 4f, (C) Nb 3d, and (D) P 2p of (a) TPANb₁, (b) Nb_{0.6}TPA, and (c) 25% TPA/Nb₂O₅ catalysts.

ions in the secondary structure of the Keggin ion. In the case of TPANb₁ catalyst band related to Lewis acidic sites was not observed which indicates the successful incorporation of Nb into the primary structure of Keggin ion. FT-IR of pyridine adsorption measurements enabled us to distinguish the incorporated of Nb either into the primary or secondary structures of TPA.

3.6. X-ray photo electron spectroscopy

XPS spectra of O 1s, P 2p, W 4f and Nb 3d of the TPANb₁, Nb_{0.6}TPA and 25% TPA/Nb₂O₅ catalysts are shown in Fig. 4. The BE values of the O 1s, P 2p, W 4f and Nb 3d for these catalysts are tabulated and presented in supplementary information (Table S1). Fig. 4(A) shows the O 1s XPS spectra of all the catalysts in the region of 530.9–533.1 eV. The BE region of O 1s is deconvoluted into two peaks. The first peak is attributed to oxygen present in M—O—M, and the second peak is ascribed to the oxygen of M—O—P of the catalyst. In the case of 25% TPA/Nb₂O₅ catalyst, first peak might be due to the oxygen present in niobia, and latter might be related to oxygen present in W—O—W and/or W—O—P [17]. In general, the O 1s spectra of oxygen attached to metal atom observed at 531 eV. In the case of terminal oxygen of M=O units, two bonds of the oxygen are attached to metal atom. Therefore the binding energy of the O 1s observed in the same region as that of W—O—W bond. Similarly in the case of supported heteropoly acid catalysts, the terminal oxygen of W=O might be interacted with the support. Fig. 4(B) shows the W 4f doublet in the range of 36.2–38.9 eV. B.E values for W 4f_{7/2} and W 4f_{5/2} were observed in the regions of 36.2–36.8 and 38.3–38.9 respectively, which are typical B.E values of W⁶⁺ oxidation state [17,21].

Fig. 4(C) shows XPS of Nb 3d in the region of 207.4–210.9 eV. The B.E in the range of 207.4–208.5 and 210.1–210.9 eV corresponds to Nb 3d_{5/2} and Nb 3d_{3/2} of Nb⁵⁺ species, respectively [22]. Presence of Nb⁵⁺ confirms the exchange of Nb ions in the primary and secondary structures of heteropoly tungstate. P 2p B.E region was deconvoluted into three peaks in the range of 133.3–135.9 eV, as shown in Fig. 4(D). The B.E values of P 2p confirms the presence of phosphorus in the form of phosphate [17,21]. The XPS results indicate that the exchanged and/or incorporated Nb is in its 5+ oxidation state.

3.7. X-ray absorption spectroscopy

In order to get more information about the nature and location of the Nb, samples were characterized by X-ray absorption spectroscopy (XAS). The normalized XANES (X-ray absorption near edge structure) of TPANb₁, Nb_{0.6}TPA, 25% TPA/Nb₂O₅ along with Nb₂O₅ are compared in Fig. 5a. k^2 -weighted Fourier transforms (FT) of EXAFS (Extended X-ray absorption fine structure) spectra in R-space are shown in Fig. 5b. Spectra of the samples in the XANES region resemble to that of bulk Nb₂O₅ reference. To explain the minute differences in the symmetry of the Nb species, we should take the pre-edge features under consideration. Generally, the presence of a pre-edge peak associated with 1s-nd transitions can be useful in determining the geometry of transition metal ions [23]. In case of Nb, the intensity of the pre-edge peak due to the 1s-4d transition discriminates the tetrahedral (Td) and octahedral geometries [24]. Intense and distinct pre-edge peak is associated to tetrahedral geometry around the absorbing atom, while in octahedral geometry this feature is much less prominent. The pre-edge features of the samples are shown as inset diagram in Fig. 5a. The less intense pre-edge (like a shoulder) in the 25% TPA/Nb₂O₅ could be associated to distorted octahedral (Oh) environment of Nb sites. Almost similar geometry can be expected in the bulk Nb₂O₅ based on the shape of pre-edge. The intensity of the pre-edge is also influenced by the adsorption of water molecule, which can able to convert the

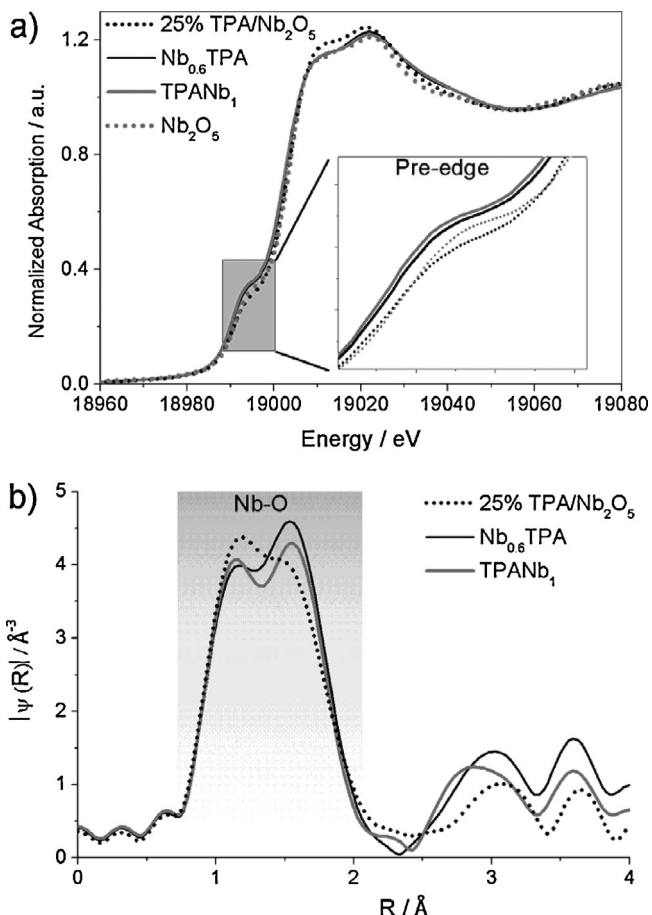


Fig. 5. (a) Normalized Nb K-edge XANES and (b) k^2 – weighted Fourier transform (FT) of TPANb₁, Nb_{0.6}TPA, 25% TPA/Nb₂O₅, and Nb₂O₅.

surface of Nb sites from tetrahedral to octahedral geometry [24]. Such interaction of water molecule from the secondary structure of Keggin ion [2] with the Nb sites in the Nb_{0.6}TPA sample might lowered the pre-edge peak compare to its counterpart (TPANb₁) catalyst. Since no water molecule exist in primary structure of TPA the pre-edge intensity of TPANb₁ is higher compare to all the samples, indicating the presence of lower oxygen atoms around Nb than in Oh. Thus, FT of the EXAFS (Fig. 5b) also shows the low amplitude for the Nb—O signal for TPANb₁ indicating low Nb—O coordination. In summary, XAS measurements revealed the nature, and locations of the Nb ion present either in the primary or secondary structures of TPA or exposed to moisture.

3.8. UV-diffused reflectance spectroscopy

Location of niobium ion was further confirmed by UV-diffused reflectance spectroscopy (Fig. 6). Polyanions exhibits a strong absorption band in the range of 200–500 nm due to oxygen-metal charge transfer [25]. Pure TPA showed a broad band that extends from 200 to 400 nm, ascribed to tungsten in octahedral coordination [26]. All the Nb containing catalysts also showed broad band corresponding to Keggin ion. However, shift in band position to higher wavelengths (Red shift) was observed in the case of TPANb₁ and Nb_{0.6}TPA catalysts. Whereas, in the case of 25% TPA/Nb₂O₅ the absorption band was shifted to lower wavelengths (389 nm) compared to TPA (Blue shift). This might be due to strong interaction of Keggin ion of TPA with niobia. In the case of Nb_{0.6}TPA catalyst, absorption band was similar to that of parent TPA but slightly extended to 415 nm (Red shift). This might be due to exchange of

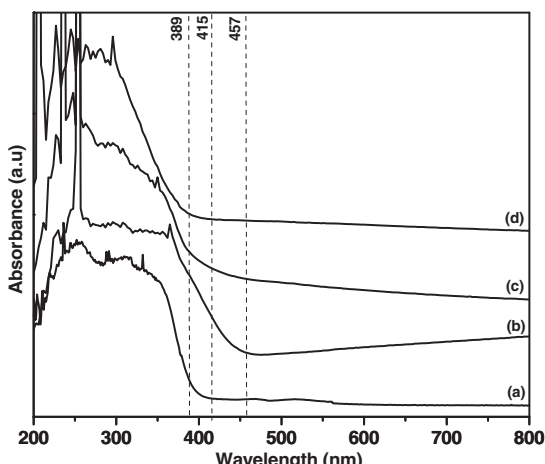


Fig. 6. UV-DRS spectra of (a) TPA, (b) TPANb₁, (c) Nb_{0.6}TPA, and (d) 25% TPA/Nb₂O₅ catalysts.

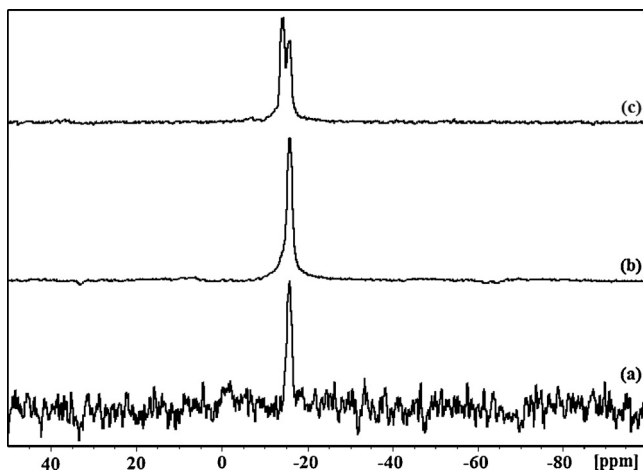


Fig. 7. ³¹P solid state NMR spectra of niobium containing heteropoly tungstate catalysts (a) 25% TPA/Nb₂O₅, (b) Nb_{0.6}TPA, and (c) TPANb₁.

protons of TPA with Nb⁵⁺ ions. Incorporation of metal ion into the secondary structure does not change the primary Keggin ion structure. The red shift was more pronounced when Nb is incorporated into the primary structure of TPA. The absorption band was broad and extended to 457 nm for TPANb₁ catalyst. These results corroborate the presence of Nb in the primary and secondary structures of the Keggin ion.

3.9. Solid state ³¹P NMR spectroscopy

Solid state ³¹P NMR spectroscopy is very sensitive method to assess the structure and stability of heteropoly acids. By using this technique one can determine purity of the heteropoly acid, degree of hydration, change in the environment around the transition metal, central atom and formation of $[\equiv M-OH_2]_n^+ [H_{3-n}PW_{12}O_{40}]^{n-3}$ species are due to interactions between the support and heteropoly acid [27–30]. Fig. 7 shows the ³¹P NMR spectra of niobium containing heteropoly tungstate catalysts. From the literature it can be noticed that ³¹P NMR signal of crystalline bulk TPA is observed at -15.5 ppm corresponding to the four co-ordinated phosphorous located in the center of the Keggin anion [22,31]. ³¹P NMR spectra of Nb_{0.6}TPA and 25% TPA/Nb₂O₅ catalysts demonstrate single peaks at -15.79 and -15.81 ppm, respectively. This indicates that exchanging the protons of heteropoly tungstate and/or supporting heteropoly

Table 2

Activity results of niobium containing heteropoly tungstate catalysts for benzylation of anisole with benzyl alcohol.

Catalyst	Conversion of benzyl alcohol (%)		Yield (%)
	Benzylanisole (<i>o</i> -, <i>p</i> -)	Ether	
25% TPA/Nb ₂ O ₅	52.8		32.2
Nb _{0.6} TPA	89.1		66.7
TPANb ₁	98.8		82.1
			20.6
			22.4
			16.7

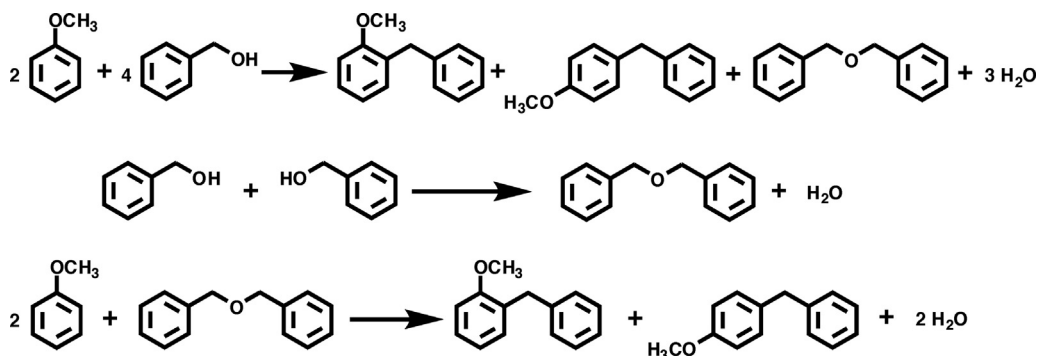
tungstate on niobia did not affect the P environment in Keggin unit and structure of the PW₁₂O₄₀³⁻ anion during the preparation of catalysts. These results are in consistent with the FT-IR and XRD results. However, TPANb₁ catalyst showed two signals in the ³¹P NMR spectra. Signal observed at -15.73 ppm can be assigned to bulk TPA [22]. Another signal with high intensity observed at -14.26 ppm is due to incorporation of Nb⁵⁺ into the primary structure, which results a change in the P environment of Keggin heteropoly tungstate. These two signals were observed due to presence of PW₁₂ and PW₁₁Nb₁ units. The ratio of PW₁₁Nb to PW₁₂ is about 1.3. The percentages of PW₁₁Nb and PW₁₂ in the sample are 56 and 44 respectively. From the elemental analysis of the TPANb₁ sample the Nb/W ratio is 0.6/11.4. As TPANb₁ sample consists of both PW₁₂ and PW₁₁Nb₁ units, therefore high content of W was observed in the sample. This chemical shift is similar to that reported by other authors [30,32]. From these results it can be noted that majority of Nb is incorporated into Keggin heteropoly acid and a small amount of TPA is also present. These results reveal the successful preparation of Nb incorporated TPA catalyst.

3.10. Evaluation of catalysts activity

The activities of the catalysts were evaluated for benzylation of anisole with benzyl alcohol and the results are shown in Table 2. In this reaction, *o*- and *p*- substituted benzylated products were obtained as major products and a side product is also formed due to dehydration reaction as shown in Scheme 2. Moderate to high yields of benzylated products were obtained for the catalysts. Both the Nb_{0.6}TPA and TPANb₁ catalysts showed high activity compared to the TPA supported on Nb₂O₅ catalyst. The TPANb₁ catalyst exhibited better activity than Nb_{0.6}TPA catalyst. The TPANb₁ catalyst showed near complete conversion with 82.1% yield towards benzylated products.

The benzylation activity of the catalysts can be correlated to their acidity. The acidity of the catalysts is largely influenced by the location of Nb in TPA. Both the Nb containing catalysts exhibited high acidity compared to supported catalyst. The benzylation activity of the catalysts is also in the same order as that of acidity. The TPANb₁ catalyst showed maximum acidity and there by high activity among all the catalysts. TPD of NH₃ results are also in good agreement with the catalytic activity of benzylation of anisole with benzyl alcohol. The characterization results revealed that the Nb is located as desired. The location of Nb is directing the properties of the catalysts. These results suggest that heteropoly tungstae can be modified to tune its catalytic properties.

The influence of benzylation agent was carried out by taking dibenzyl ether as benzylation agent. In dehydration reaction, two moles of benzyl alcohol yields one mole of dibenzyl ether as shown in Scheme 2. In order to compare the influence of benzylation agent, the amount of dibenzylether was taken as half of the moles of benzyl alcohol. The activity results of niobium containing catalysts for benzylation of anisole with dibenzyl ether at a reaction time of 30 min are shown in Table 3. In this case also the Nb containing catalysts performance was high compared to 25% TPA/Nb₂O₅ catalyst. Dibenzylether conversion up to 87.8% with 86.2% of yield towards benzylated products was observed for TPANb₁ catalyst.



Scheme 2. Reaction scheme for the benzylation of anisole with benzyl alcohol and dibenzyl ether as benzylating agents.

Table 3

Activity results of niobium containing heteropoly tungstate catalysts for benzylation of anisole with dibenzyl ether.

Catalyst	Conversion of dibenzyl ether (%)	Yield (%)	
		Benzylanisole (<i>o</i> -, <i>p</i> -)	Benzyl alcohol
25% TPA/Nb ₂ O ₅	43.6	38.5	5.1
Nb _{0.6} TPA	68.1	62.5	5.6
TPANb ₁	87.8	86.2	1.6

In the benzylation of anisole reaction, highest conversion with in less reaction time was observed by using benzyl alcohol as benzylating agent compared to dibenzylether. TPANb₁ catalyst showed about 87.8% conversion of dibenzylether with in 30 min of reaction time, whereas in the case of benzyl alcohol 98.8% of conversion was observed within 15 min. The high benzyl alcohol conversion can be explained by the adsorption of benzylating agent on to the catalyst surface. Adsorption of benzyl alcohol molecule on the catalyst surface is easier than that of dibenzylether molecule as the later is a bulky molecule.

4. Conclusions

The catalysts with incorporation of niobium in the primary and secondary structure of heteropoly tungstate were successfully prepared with retention of Keggin structure. These catalysts showed high activity for liquid phase benzylation of anisole with benzyl alcohol and dibenzyl ether as benzylating agents. The characteristics of catalysts depended on the location of Nb in heteropoly tungstate. Incorporation of niobium into primary structure of heteropoly tungstate resulted in high acidity. HPAs catalytic properties can be tuned by modifying with metal ion both in the primary and secondary structures of Keggin ion. The benzylation activity of the catalysts depended on their acidities. The benzylation of anisole also depends on the benzylating agent.

Acknowledgements

ChRK thank Council of Scientific & Industrial Research, India for financial assistance in the form of Junior & Senior Research Fellowships.

Appendix A. Supplementary data

Supplementary data associated with this article can be found, in the online version, at <http://dx.doi.org/10.1016/j.apcata.2015.06.023>.

References

- [1] M.T. Pope, A. Muller, Angew. Chem. Int. Ed. Engl. 30 (1991) 34–48.
- [2] M. Misono, Chem. Commun. (2001) 1141–1152.
- [3] I.V. Kozhevnikov, Catalysts for Fine Chemical Synthesis: Catalysis by Polyoxometalates, vol. 2, Wiley, 2002, pp. 81.
- [4] I.V. Kozhevnikov, Catal. Rev. Sci. Eng. 37 (1995) 311–352.
- [5] I.K. Song, M.A. Barreau, Korean J. Chem. Eng. 19 (2002) 567–573.
- [6] M.H. Youn, D.R. Park, J.C. Jung, H. Kim, M.A. Barreau, I.K. Song, Korean J. Chem. Eng. 24 (2007) 51–54.
- [7] D.R. Park, S.H. Song, U.G. Hong, J.G. Seo, J.C. Jung, I.K. Song, Catal. Lett. 132 (2009) 363–369.
- [8] D.R. Park, S. Park, Y. Bang, I.K. Song, Appl. Catal. A 373 (2010) 201–207.
- [9] D.R. Park, U.G. Hong, S.H. Song, J.G. Seo, S.H. Baek, J.S. Chung, I.K. Song, Korean J. Chem. Eng. 27 (2) (2010) 465–468.
- [10] N. Lingaiah, J.E. Molinari, I.E. Wachs, J. Am. Chem. Soc. 131 (2009) 15544–15554.
- [11] D. Casarini, G. Centi, P. Jiru, V. Lena, Z. Tvaruzkova, J. Catal. 143 (1993) 325–344.
- [12] Y. Seki, N. Mizuno, M. Misono, J. Mol. Catal. A 194–195 (2000) 13–20.
- [13] S. Shinzaki, M. Matsushita, K. Yamaguchi, N. Mizuno, J. Catal. 233 (2005) 81–89.
- [14] Ch. Ramesh Kumar, M. Srinivas, N. Lingaiah, Appl. Catal. A 487 (2014) 165–171.
- [15] E. Caliman, J.A. Dias, S.C.L. Dias, F.A.C. Garcia, J.L. de Macedo, L.S. Almeida, Micropor. Mesopor. Mater. 132 (2010) 103–111.
- [16] Ch. Ramesh Kumar, K.T. Venkateswara Rao, P.S. Sai Prasad, N. Lingaiah, J. Mol. Catal. A 337 (2011) 17–24.
- [17] Ch. Ramesh Kumar, K. Jagadeeswaraiah, P.S. Sai Prasad, N. Lingaiah, ChemCatChem 4 (2012) 1360–1367.
- [18] C. Tiozzo, C. Bisio, F. Carniato, A. Gallo, S.L. Scott, R. Psaro, M. Guidotti, Phys. Chem. Chem. Phys. 15 (2013) 13354–13362.
- [19] M.A. Vuurman, I.E. Wachs, A.M. Hirt, J. Phys. Chem. 95 (1991) 9928–9937.
- [20] Ch. Ramesh Kumar, N. Rambabu, N. Lingaiah, P.S. Sai Prasad, A.K. Dalaia, Appl. Catal. A 471 (2014) 1–11.
- [21] Ch. Ramesh Kumar, P.S. Sai Prasad, N. Lingaiah, J. Mol. Catal. A 350 (2011) 83–90.
- [22] C.G. Sancho, R.M. Tost, J.M.M. Robles, J.S. Gonzalez, A.J. Lopez, P.M. Torres, Appl. Catal. B 108–109 (2003) 161–167.
- [23] J.A. Horsley, I.E. Wachs, J.M. Brown, G.H. Via, F.D. Hardcastle, J. Phys. Chem. 91 (15) (1987) 4014–4020.
- [24] S. Yoshida, T. Tanaka, T. Hanada, T. Hiraiwa, H. Kanai, T. Funabiki, Catal. Lett. 12 (1992) 277–286.
- [25] G. Romanelli, J.C. Autino, P. Vazquez, L. Pizzio, M. Blanco, C. Caceres, Appl. Catal. A 352 (2009) 208–213.
- [26] G. Romanelli, P. Vazquez, L. Pizzio, N. Quaranta, J. Autino, M. Blanco, C. Caceres, Appl. Catal. A 261 (2004) 163–170.
- [27] F. Su, L. Ma, Y. Guo, W. Li, Catal. Sci. Technol. 2 (2012) 2367–2374.
- [28] V. Dufaud, F. Lefebvre, Materials 3 (2010) 682–703.
- [29] L. Matachowski, A. Drelinkiewicz, E. Lalik, D. Mucha, B. Gil, Z.B. Mucha, Z. Olejniczak, Micropor. Mesopor. Mater. 144 (2011) 46–56.
- [30] K. Okumura, K. Yamashita, K. Yamada, M. Niwa, J. Catal. 245 (2007) 75–83.
- [31] T. Okuhara, H. Watanabe, T. Nishimura, K. Inumaru, M. Misono, Chem. Mater. 12 (2000) 2230–2238.
- [32] M. Caiado, A. Machado, R.N. Santos, I. Matos, I.M. Fonseca, A.M. Ramos, J. Vital, A.A. Valente, J.E. Castanheiro, Appl. Catal. A 451 (2013) 36–42.